Recombinant expression and characterization of *GSTd3* from a resistant population of *Anopheles arabiensis* and comparison of DDTase activity with *GSTe2*

Xueping Lu[1], Eba Alemayehu Simma[2], Pieter Spanoghe[1], Thomas Van Leeuwen[1], Wannes Dermauw[1,3]

[1]Department of Plants and Crops, Faculty of Bioscience Engineering, Ghent University, Coupure links 653, 9000, Ghent, Belgium

[2]Department of Biology, College of Natural Sciences, Jimma University, Jimma, Ethiopia

[3]Flanders Research Institute for Agriculture, Fisheries and Food (ILVO), Plant Sciences Unit, 9820 Merelbeke, Belgium

Corresponding author: Wannes.Dermauw@ilvo.vlaanderen.be; thomas.vanleeuwen@ugent.be

Abstract

The development of insecticide resistance in malaria vectors is a challenge for the global effort to control and eradicate malaria. Glutathione S-transferases (GSTs) are multifunctional enzymes involved in the detoxification of many classes of insecticides. For mosquitoes, it is known that overexpression of an epsilon GST, *GSTe2,* confers resistance towards DDT and pyrethroids. In addition to *GSTe2*, consistent overexpression of a delta class GST, *GSTd3*, has been observed in insecticide resistant populations of different malaria vector species. However, the functional role of GSTd3 towards DDT resistance has not yet been investigated. Here, we recombinantly expressed both *GSTe2* and *GSTd3* from *Anopheles arabiensis* and compared their metabolic activities against DDT. Both AaGSTd3 and AaGSTe2 exhibited CDNB-conjugating and glutathione peroxidase activity and DDT metabolism was observed for both GSTs. However, the DDT dehydrochlorinase activity exhibited by AaGSTe2 was much higher than for AaGSTd3, and AaGSTe2 was also able to eliminate DDE although the metabolite could not be identified. Molecular modeling revealed subtle differences in the binding pocket of both enzymes and a better fit of DDT within the H-site of AaGSTe2. The overexpression but much lower DDT metabolic activity of AaGSTd3, might suggest that AaGSTd3 sequesters DDT. These findings highlight the complexity of insecticide resistance in the major malaria vectors and the difficulties associated with control of the vectors using DDT, which is still used for indoor residual spraying.

Keywords*: Anopheles arabiensis*, GSTd3, GSTe2*,* DDTase activity, insecticide resistance

1. Introduction

Malaria is a mosquito-borne disease that has affected humans for thousands of years. During the last decades, several interventions, mainly chemical based vector control, have been implemented to combat malaria. As a result, the number of malaria deaths has been reduced to 568,000 in 2019, while in 2020, malaria deaths slightly increased by 12% due to the COVID-19 pandemic and remained stable in 2021 (WHO, 2022). The reduction of malaria mortality and morbidity in the last decade is mainly due to indoor residual spraying (IRS) and the use of long-lasting insecticidal nets (LLINs) (Dhiman, 2019; WHO, 2022). However, insecticide resistance of malaria vectors to at least one of the commonly-used insecticide classes has been reported in 78 countries and is a challenge for the global efforts to control and eradicate malaria (WHO, 2022). More specifically, the widespread insecticide resistance in the major malaria vector species of the *Anopheles gambiae* complex (*An. coluzzii, An. gambiae sensu stricto* and *An. arabiensis*) and *An. funestus* jeopardize malaria control and elimination strategies (Antonio-Nkondjio et al., 2017; Hancock et al., 2020; Kleinschmidt et al., 2018; Matiya et al., 2019; Wiebe et al., 2017). In addition to widespread resistance, the invasion of *Anopheles stephensi*, native to southern and western Asia, into cities of eastern Africa makes it also more difficult to control malaria vectors (Takken and Lindsay, 2019).

In general, resistance is either caused by mutations in the gene encoding the target site of insecticides (toxicodynamic resistance) and/or by decreased exposure (pharmacokinetic resistance) due to quantitative or qualitative changes in major detoxification enzymes and transporters, such as cytochrome P450 monooxygenases (P450s), carboxyl/cholinesterases, glutathione S-transferases (GSTs) and ABC transporters (Feyereisen et al., 2015; Hemingway and Ranson, 2000). The most common target site mutation known to confer resistance against pyrethroids and DDT is the *k*nock*d*own *r*esistance (*kdr*) mutation in the voltage-gated sodium channel (VGSC) gene, resulting in a leucine to phenylalanine (L1014F) or a leucine to serine (L1014S) substitution at position 1014 (Liu, 2015; Silva et al., 2014). On the other hand, P450s, such as CYP6M2, CYP6P3 and/or CYP6P4, and GSTs are well-known for their role in pyrethroid and DDT metabolism (Müller et al., 2008; Riveron et al., 2017; Riveron et al., 2014b; Stevenson et al., 2011).

Insect GSTs catalyze the detoxification of several major classes of insecticides through glutathione conjugation, dehydrochlorination or passive binding, or protect insects against oxidative damage caused by insecticides via glutathione peroxidase activity (Abel et al., 2004; Hayes and Wolf, 1988; Mannervik et al., 1988; Pickett and Lu, 1989; Wongtrakul et al., 2014; Yang et al., 2001). Glutathione-based dehydrochlorination of

the organochlorine compound DDT has been reported to confer resistance in *Aedes aegypti*, *An. dirus* and *An. gambiae*, but is also a common detoxification mechanism in other insects (Clark and Shamaan, 1984; Clark et al., 1986; Enayati et al., 2005; Grant et al., 1991; Lumjuan et al., 2005; Ortelli et al., 2003; Pavlidi et al., 2018; Prapanthadara et al., 1995; Prapanthadara et al., 1996; Prapanthadara et al., 2000; Prapanthadara et al., 1993; Ranson et al., 2001; You et al., 2015). Mosquito GSTs have also been reported to play a role in the sequestration and/or detoxification of pyrethroids and glutathione peroxidase activity of GSTs has been detected in *An. gambiae, An. cracens*, *Ae. aegypti* and other insects (Kostaropoulos et al., 2001; Lumjuan et al., 2005; Ortelli et al., 2003; Sawicki et al., 2003; Singh et al., 2001; Vontas et al., 2001; Wongtrakul et al., 2014).

Cytosolic GSTs are grouped into eight classes: delta, epsilon, omega, sigma, theta, zeta, xi and iota, with delta and/or epsilon classes being only present in mites or insects (Che-Mendoza et al., 2009; Ding et al., 2003; Ranson et al., 2002; Ranson et al., 2001; Tu and Akgül, 2005). Delta and epsilon GSTs were previously shown to play a vital role in resistance to insecticides in different species of Diptera and metabolism of DDT in *An. gambiae*, *Culex quinquefasciatus* and *Ae. aegypti* has been linked to increased epsilon class GST dehydrochlorinase activity (Ding et al., 2003; Hemingway et al., 2004; Lumjuan et al., 2011; Lumjuan et al., 2007; Ortelli et al., 2003; Polson et al., 2011; Prapanthadara et al., 2000; Ranson et al., 1997; Ranson et al., 2001). Twenty-eight cytosolic GST genes were identified in the *An. gambiae* genome, and 12 and 8 of these genes encode delta and epsilon GSTs, respectively (Strode et al., 2008). Of the eight *An. gambiae* epsilon GSTs, the *GSTe2* gene is most conserved and consistently associated with DDT and, to a lower extent, pyrethroid resistance (Ayres et al., 2011; Djouaka et al., 2011; Lumjuan et al., 2005; Lumjuan et al., 2011; Mitchell et al., 2014; Ortelli et al., 2003). For example, GSTe2 is also thought to metabolize the pyrethroid permethrin in *An. funestus*, although the nature of the permethrin metabolites has not been identified yet (Riveron et al., 2014b).

Genes that were overexpressed in resistant *An. arabiensis* populations from Ethiopia have been recently identified by RNAseq analysis and, amongst others, included a delta GST gene, *GSTd3* (Messenger et al., 2021; Simma et al., 2019). *GSTd3* overexpression has been reported earlier for several pyrethroid/DDT resistant anopheline populations (Table S1). However, in contrast to GSTe2, the contribution of GSTd3 to DDT resistance has not yet been studied. Here, we functionally characterized *An. arabiensis* *GSTd3* and investigated the potency of GSTd3 to metabolize DDT in comparison with GSTe2.

2. Materials and Methods

2.1. Expression of *GSTd3* in DDT resistant anopheline mosquito populations

2.1.1. RT-qPCR of *GSTd3* in DDT resistant *An. arabiensis* populations from Ethiopia

The DDT and deltamethrin resistant *An. arabiensis* populations from Ethiopia [Asendabo (ASN), Chewaka (CHW), and Tolay (TOL)] and the Ethiopian susceptible population Sekoru (SEK) have been previously described .(Alemayehu et al., 2017; Simma et al., 2019). RNA was extracted from these populations, and stored at -80 °C until further use, as described in Simma et al. 2019. RNA was reverse transcribed using the Maxima First Strand cDNA synthesis for RT-qPCR kit [Fermentas (Thermo Fisher Scientific), Belgium] using 2 µg of total RNA as the template according to the protocol. The RT-qPCR reactions were performed on a Mx3005P qPCR system [Stratagene (Agilent Technologies), Belgium)] using the Maxima SYBR Green qPCR master mix with ROX solution [Fermentas (Thermo Fisher Scientific), Belgium] according to the manufacturer's instructions. The optimized qPCR program was an initial denaturation at 95 °C for 10 min, followed by 35 cycles of 95 °C for 15 s, 55 °C for 30 s and 72 °C for 30 s. At the end, a melting curve was constructed by ramping from 65 °C to 95 °C, at 1 °C per 2 s. RT-qPCR primers for *GSTd3* as well as for reference genes, *40S ribosomal protein S7* (*RpS7*) and *elongation factor Tu* (*EF-Tu*) can be found in Table S2. All qPCR experiments were conducted using four biological and two technical replicates. Relative expression levels and significant gene expression differences (independent t-test) were calculated with qbase+2 (Biogazelle, Zwijnaarde, Belgium - www.qbaseplus.com) and SPSS 28 (IBM, USA).

2.1.2. Expression levels of *GSTe2* and *GSTd3* in other anopheline mosquito populations

Relative *GSTd3* (VectorBase ID: AGAP004382 for *An. gambiae* and AARA015764 for *An. arabiensis*) and *GSTe2* (VectorBase ID: AGAP009194 for *An. gambiae*, AARA008732 for *An. arabiensis*) expression data were obtained from previous reports, using the IR-TEx database as a guidance (http://opteron.lstmed.ac.uk/shiny/IR-TEx/) (Ingham et al., 2018). In addition, the Google scholar database was mined for studies using the keywords "mosquitoes" and "*GSTd3*".

2.2. Analyzing *AaGSTd3* and *AaGSTe2* sequences of the DDT resistant TOL population

Based on a previously published RNAseq dataset (Simma et al., 2019), we compared the *AaGSTd3* CDS between the DDT and deltamethrin resistant TOL population and

160 the susceptible SEK population. The *AaGSTd3* CDS of the TOL population was also
161 compared against the *An. arabiensis* reference (Dongola) strain in VectorBase. The
162 *AaGSTe2* CDS of the TOL population was PCR amplified using primers listed in Table
163 S2. PCR amplification was performed on newly synthesized cDNA from the TOL
164 population using GoTaq G2 DNA Polymerase (Promega, Belgium) and the following
165 conditions: 1 cycle at 95 °C for 2 min; 35 cycles of 95 °C for 30s, 55 °C for 30s and
166 72 °C for 60 s; and 1 cycle at 72 °C for 5 min. The PCR products were purified using
167 the E.Z.N.A Cycle Pure Kit (Omega Bio-Tek, Belgium) and then sequenced (LGC
168 Genomics, Germany). The obtained *AaGSTe2* CDS of the TOL population was
169 compared against the *An. arabiensis* reference (Dongola) strain and the *An. gambiae*
170 reference (PEST) strain in VectorBase (Lawson et al., 2009).

171

2.3. Functional expression of *AaGSTd3* and *AaGSTe2 in vitro* and protein purification

174 The *GSTd3* CDS of the *An. arabiensis* reference strain (AARA015764-RA at
175 VectorBase) and *GSTe2* CDS of the *An. arabiensis* TOL population were used for
176 protein expression. GST CDS were codon optimized for expression in *E. coli*,
177 synthesized including a C-terminal 6x His-tag, and cloned into a pet-30a+ expression
178 vector by Genscript (Piscataway, NJ, USA) (see Table S3 for codon optimized
179 sequence of *AaGSTd3* and *AaGSTe2*). Expression plasmids were first transformed into
180 a non-expression host, *E. coli* DH5α [Fermentas (Thermo Fisher Scientific), Belgium].
181 Purified plasmids were then sequenced to confirm sequence integrity (LGC Genomics,
182 Germany). After transformation into the expression host, *E. coli* BL21 (DE3)
183 competent cells (New England Biolabs, Belgium), a single colony containing
184 recombinant plasmid was grown in 20 ml of LB low salt medium containing kanamycin
185 at 37 °C overnight. This culture was used to inoculate 1000 ml LB low salt medium
186 and grown until the OD600 reached 0.8 at 37 °C. Expression was induced by adding
187 0.3 mM isopropyl β-D-thiogalactoside (IPTG) followed by an additional incubation at
188 28 °C for 20 h. The cells were harvested by centrifugation at 4000 rpm for 20 min,
189 freeze-thawed, re-suspended in 80 ml cell lysis buffer containing 0.1 M sodium
190 phosphate buffer (pH 7.4), 0.5 M sodium chloride, 10 mM imidazole, 2% glycerol, and
191 0.14% mercapto-ethanol and disrupted by sonication for 30 min using 5 s bursts at low
192 intensity (25%) with a 5 s cooling period between each burst on ice. Cell lysates were
193 centrifuged at 7000 g at 4 °C for 30 min in a rotor to pellet the cellular debris and the
194 supernatant was used for the purification. Purification was performed via Ni-NTA
195 Agarose (Qiagen, Belgium) to purify recombinant proteins containing a 6x His-tagged
196 sequence according to the manufacturer's instructions. Briefly, one ml of resin was

pipetted into a 10-ml column and, subsequently, this column was pre-equilibrated with 10 ml 100 mM PBS (pH 7.4). The supernatant was then loaded on the column, unbound proteins were washed by 10 ml wash buffer consisting of 100 mM PBS (pH 7.4), 500 mM NaCl, and a series of imidazole concentrations (20, 25 and 50 mM). Recombinant proteins were collected by adding 75 and 100 mM imidazole. The 10-kDa cutoff Pierce™ Protein concentrator [Fermentas (Thermo Fisher Scientific), Belgium] was used to remove imidazole and NaCl and to obtain a higher concentration of protein.

Protein concentration was measured with the Bradford assay and the quality of the samples was monitored by sodium dodecyl sulfate-polyacrylamide gel electrophoresis (SDS-PAGE) and Western blotting as previously described (Bradford, 1976; Wybouw et al., 2012).

2.4.   Determination of enzyme activity

Glutathione peroxidase activity with cumene hydroperoxide (CHP) was determined using the method of Samra et al. (2012). Briefly, the reaction systems in UV-STAR 96-well microplates (Greiner bio-one, Belgium) comprised 100 mM potassium phosphate buffer (pH 6.5), 2 µg AaGSTd3 or AaGSTe2, 1 mM cumene hydroperoxide (CMHP), 2 units of glutathione reductase from baker's yeast, 7.5 mM reduced Glutathione (GSH), 0.3 mM NADPH (all obtained from Sigma-Aldrich, Belgium). After incubation at 30 °C for 5 min, CMHP was added to initiate the reaction. The oxidation of NADPH was measured at 15 s intervals at A_{340} for 5 min. Wells lacking enzyme but containing all of the substrates served as blanks. The assays were performed in quadruplicate and repeated 3 times using a Biotek EON microplate spectrophotometer (Biotek, France).

GST activity against the model substrates 1-chloro-2, 4-dinitrobenzene (CDNB) and 1,2-dichloro-4-nitrobenzene (DCNB) (Sigma-Aldrich, Belgium) was measured at 30 °C in clear UV-STAR 96-well microplates (Greiner bio-one, Belgium) according to the method of Habig et al. (1974). CDNB and DCNB were dissolved in ethanol first and then diluted with 100 mM potassium phosphate buffer (pH 6.5), while reduced GSH was dissolved in 100 mM potassium phosphate buffer (pH 6.5). The activity with 1 mM CDNB or DCNB and 5 mM reduced glutathione in 300 µl was measured at A_{340} for 5 min at 15 s intervals using a Biotek EON microplate spectrophotometer. Wells containing all reagents except enzyme served as control. The assays were performed in quadruplicate and repeated 3 times. Significant differences were tested using an independent t-test.

2.5.   Kinetic studies

The steady-state kinetic parameters of GST activity were determined for the CDNB conjugating reaction by using varying concentration of CDNB and keeping the GSH

233   concentration fixed and vice versa. For AaGSTd3, the initial rates were determined in

234   the presence of 2 mM GSH and varying concentrations of CDNB (0.01-2.5 mM), while

235   at 2 mM of CDNB, GSH was used in the concentration range 0.6-10 mM. The assays

236   were performed with 0.8 µg of AaGSTd3 in 100 mM potassium phosphate buffer at

237   30 °C (pH 6.5). For AaGSTe2, the initial rates were determined in the presence of 10

238   mM GSH and varying concentrations of CDNB (0.0025-1 mM), while CDNB was used

239   at a fixed concentration of 1mM when GSH was used in the concentration range 0.416-

240   20 mM. The assays were performed with 50 ng of AaGSTe2 in 100 mM potassium

241   phosphate buffer at 30 °C (pH 6.5). Reactions containing all reagents except

242   recombinant enzyme served as control. The assays were performed in quadruplicate

243   and repeated 3 times. The assays were performed as described above in section 2.3. The

244   kinetic constants were determined by fitting the Michaelis-Menten equation or Hill

245   equation using SigmaPlot (Systat Software Inc., San Jose, CA). Significant differences

246   were tested using an independent t-test.

2.6. Determination of DDT dehydrochlorinase activity using gas chromatography with electron capture detection (GC-ECD)

249   The DDT dehydrochlorinase (DDTase) activity of AaGSTd3 and AaGSTe2 was

250   assessed using metabolic assays and confirmed with gas chromatography with an

251   electron capture detector, GC-ECD (Agilent Technologies 6890 N) (see below) as

252   previously described with some modifications (Mekonen et al., 2015). Metabolic assays

253   were conducted at 30 °C for 6, 12, 24 and 36h while shaking at 150 rpm (Labnet 311DS)

254   (Samra et al., 2012; Tao et al., 2022). The reaction system comprised 100 mM

255   potassium phosphate buffer (pH 6.5), 10 mM GSH, 300 µg AaGSTd3 or AaGSTe2,

256   and 3.4 µM 4,4'-DDT [PESTANAL® analytical standard with purity $\geq$ 98.0%; Sigma-

257   Aldrich (Belgium) product number 31041] in acetone (the final concentration of

258   acetone in the reaction system was 1.2%), in a total volume of 1 ml, which was carried

259   out in 7 ml Supelco vials (Sigma-Aldrich, Belgium). Control samples contained the

260   same reagent mixture with the boiled recombinant enzyme (90 °C for 10 min) or the

261   same reagent mixture without GSH. Samples with only 4,4'-DDT or 4,4'-DDE

262   [PESTANAL® analytical standard with purity $\geq$ 98.0%; Sigma-Aldrich (Belgium)

263   product number 35487] in acetone, and 100 mM potassium phosphate buffer were used

264   to evaluate recovery efficiency for each time point. Four replicates were assessed for

265   each time point and for each GST.

266   After the reaction, 4 mL of 100 mM potassium phosphate buffer (pH 6.5) was added to

267   the reaction volume to analyze DDT and possible DDT metabolites. A validated

268   analytical method was used. DDT and its possible metabolites were extracted using a

269   liquid-liquid extraction method from the water phase into the hexane phase by adding

270   5 mL hexane and then shaking by hand for at least 3 min. Hexane solutions were dried

with anhydrous Na_2SO_4 and were transferred to glass vials. The compounds were detected using an Agilent 6890N Network gas chromatograph with an auto-sampler, coupled to an electron capture detector (Agilent Technologies, Belgium). Separation was performed on a HP-5MS (5% phenyl methyl siloxane) capillary column (30 m length × 0.25 mm internal diameter, 0.25 µm film thickness) (Model number Agilent 19091 J-433). The operating conditions were as follows: The column was initially set at a temperature of 60 °C, then increased at a rate of 20 °C/min to 150 °C. It was further increased at a rate of 15 °C/min to 250 °C and held constant for 2 min, followed by an increase at a rate of 30 °C/min to 270 °C and held constant for 10 min. It was finally increased at a rate of 30 °C/min to 280 °C and held constant for 11 min. The temperature of the injector and detector were maintained at 200 °C and 250 °C, respectively. Helium was used as a carrier gas at a flow rate of 20 mL/min, and the injections were made in the split mode with a split ratio of 52.7:1. The Agilent GC ChemStation version Rev. A.10.02 software was used for system control and data acquisition and analysis. The quantities of DDT and DDE were calculated with an external standard.

The recovery efficiency was calculated based on the theoretical amount of DDT/DDE and used to calculate the concentration of DDT and DDE in control and treatment samples, to compensate for the loss during the extraction. The amount of DDE in a DDT sample was subtracted for the calculation of newly formed DDE as the standard 4,4'-DDT is not 100% pure (purity ≥ 98.0%, see above). The DDTase activity is expressed as nmol of DDE formation/mg of enzyme protein (Che-Mendoza et al., 2009; Udomsinprasert et al., 2005).

2.7.   Protein modeling and molecular docking

A structural model for AaGSTd3 was predicted using the Swiss-model server (http://swissmodel.expasy.org/) using the protein sequence of AaGSTd3 from the TOL population (identical to GSTd3 of the *An. arabiensis* reference (Dongola) strain). The crystal structure of GST1-6 from *Anopheles dirus* species B (PDB code: 1v2a.1.B) was automatically selected by the server as the most suitable template for model construction, with 85% sequence identity and with the sequence diversity being mainly located at the C-terminal domain. The model revealed a global model quality estimation (GMQE) score of 0.93. The model was also evaluated by SAVES V5.0 (http://servicesn.mbi.ucla.edu/SAVES/) and ProQ (http://prop.bioinfo.se/cgi-bin/ProQ/ProQ.cgi). Molecular docking was performed using the Swiss-Dock server and the EADock DSS (http://www.swissdock.ch/) software. The crystal structure of *An. dirus* GST1-6 has glutathione sulfonic acid (GTS) as a cofactor instead of GSH, which did not allow to predict GSH as a cofactor of AaGSTd3 using Swiss Model server (Udomsinprasert et al., 2005). Hence, molecular docking simulation needed to be

performed for both DDT and GSH for AaGSTd3. The binding modes were generated via the blind docking method to check the possibility for all target cavities. The Chemistry at HARvard Macromolecular Mechanics (CHAEMM) energies were estimated using empirical energy functions, then binding modes were evaluated with Fast Analytical Continuum Treatment of Solvation (FACTS) based on the fully analytical evaluation of the volume and spatial symmetry of the solvent (Brooks et al., 1983; Haberthür and Caflisch, 2008). The model and docking results were visualized using PyMOL v2.0.7 software (DeLano, 2002). A structural model for AaGSTe2 from the TOL population was predicted using the Swiss-model server and the crystal structure of GSTe2 ZAN/U variant from *Anopheles gambiae* (PDB code: 4gsn.1). The GMQE score was 0.99. The crystal structure of *An. gambiae* GSTe2 ZAN/U has two GSH ligands as a cofactor and, using Swiss Model server, allowed to predict GSH as a cofactor of AaGSTe2 (Mitchell et al., 2014). Hence, for AaGSTe2, molecular docking simulation only needed to be performed for DDT. DDT docking and visualization was performed as described for AaGSTd3.

3. Results

3.1. *AaGSTd3* is overexpressed in DDT resistant anopheline mosquito populations

A previous RNAseq study, showed that *GSTd3* was overexpressed in DDT-resistant *An. arabiensis* populations ASN, CHW, and TOL (Simma et al., 2019) and *GSTd3* overexpression was evaluated in this study using RT-qPCR. *AaGSTd3* is 3.7, 2.5, and 3.5-fold overexpressed in ASN, CHW, and TOL compared to the DDT-susceptible population SEK ($P < 0.05$) (Figure S1).

Based on a literature search, *GSTd3* is also commonly overexpressed in other resistant anopheline mosquito populations (Fossog Tene et al., 2013; Ibrahim et al., 2022; Ingham et al., 2018; Isaacs et al., 2018; Jones et al., 2012; Kouamo et al., 2021; Nardini et al., 2012; Riveron et al., 2014a; Riveron et al., 2017; Samb et al., 2016; Simma et al., 2019; Tchigossou et al., 2018; Toé et al., 2015; Wipf et al., 2022). Among 50 exposed and unexposed anopheline populations that were resistant to DDT, RNAseq analysis revealed that *GSTd3* was overexpressed in 37 populations while both *GSTd3* and *GSTe2* were overexpressed (fold change > 2) in 19 populations (Figure 1, Table S1). Noteworthy, *GSTd3* was also overexpressed in some malathion and/or pyrethroid resistant populations where the resistance level to DDT was unknown (Table S1).

3.2. *AaGSTd3* and *AaGSTe2* sequence of the DDT resistant TOL population

The *An. arabiensis GSTd3* CDS of the DDT and deltamethrin resistant TOL population did not show non-synonymous nucleotide polymorphisms compared to the susceptible SEK population and the *An. arabiensis* reference (Dongola) strain (data not shown). However, the *An. arabiensis GSTe2* CDS of the TOL population did show three non-synonymous nucleotide polymorphisms compared to the *An. arabiensis* reference (Dongola) strain (G61A, G139T and G461C resulting in A21T, V47L, and S154T), while two non-synonymous polymorphisms were found compared to *GSTe2* of the *An. gambiae* reference (PEST) strain (C9G and G139T, resulting in N3K and V47L) (Figure S2 and Table S4).

3.3. Heterologous expression and purification of *AaGSTd3* and *AaGSTe2*

AaGSTd3 and *AaGSTe2* were expressed using *E. coli* and successfully purified, as verified by both SDS-PAGE and Western blot (Figure S3). For both AaGSTd3 and AaGSTe2, a single band at 25 kDa was observed, which is approximately the expected molecular weight of these proteins (including the C-terminal His tag). The yield of recombinant AaGSTd3 and AaGSTe2 was about 40 mg protein /L LB broth.

3.4. Substrate specificities for model substrates and kinetic parameters

Both AaGSTd3 and AaGSTe2 displayed CDNB-conjugating activity and glutathione peroxidase activity as measured by the GSH-dependent reduction of CHP. However, the activity towards model substrates was higher for AaGSTe2 (Table 1) and also the glutathione peroxidase activity was threefold higher when compared to AaGSTd3.

Analysis of Michaelis-Menten kinetics revealed that CDNB is a better substrate for recombinant AaGSTe2 than for recombinant AaGSTd3, as evidenced by the higher V_{max} and k_{cat} values and lower K_m^{CDNB}. The K_m^{CDNB} value of AaGSTd3 is 136-fold higher than the value of AaGSTe2, while the K_m^{GSH} value for recombinant AaGSTe2 was higher than for recombinant AaGSTd3 (Table 2).

3.5. AaGSTd3 and AaGSTe2 exhibited DDT dehydrochlorinase activity

The recovery of DDT and DDE after extraction ranged between 100% and 112% or between 82% and 106%, respectively, with an average of $104 \pm 3\%$ or $96 \pm 5\%$. DDT metabolism was observed for both AaGSTd3 and AaGSTe2. However, the DDTase activity of AaGSTe2 (100% DDT depletion after 6 h reaction in the presence of the cofactor GSH) was much higher than AaGSTd3 (7.4% DDT depletion after 6 h reaction in the presence of the cofactor GSH). For AaGSTd3, the amount of DDE increased over time while the amount of DDT decreased over time (DDTase activity was 0.36 ± 0.01, 0.75 ± 0.04, 1.01 ± 0.07, and 1.34 ± 0.15 nmol of DDE formation per mg protein at 6, 12, 24, and 36 h). However, for AaGSTe2, at 6 h, only very few DDE

378 was left and no DDT was detected. After 6h incubation, neither DDT nor DDE were

379 detected (Figure 2A, B, E, F). Control assays with no GSH or denatured recombinant

380 AaGSTd3 had no detectable DDE production. However, control assays with no GSH

381 but with AaGSTe2 did show DDTase activity albeit at lower rate (DDTase activity

382 was 1.55 ± 0.20, 3.69 ± 0.09, 4.58 ± 0.21, and 6.28 ± 0.11 nmol of DDE formation per

383 mg at 6, 12, 24, and 36 h) (Figure 2C, D, E, F). Values are shown as mean $\pm$ SE.

384 **3.6.   Prediction of AaGSTd3 and AaGSTe2 structures and docking of DDT**

385 The predicted monomer of AaGSTd3 were divided into two distinct domains. The C-

386 terminal domain (residues 86-210) consisted of 5 α-helices (H4-H8) in which the long

387 α-helix H4 was not significantly bent (Figure 3, 4A). The active site can be further

388 divided into a co-factor GSH-binding site (G-site), where one GSH molecule was bound,

389 and a neighboring substrate-binding site (H-site), which recognizes the hydrophobic

390 substrate. The predicted G-site in AaGSTd3 was mainly formed by Glu63, Ser64,

391 Lys105, and Lys127 with hydrogen bonds, which were hydrophilic in nature. These

392 four hydrogen bonds possibly form a three-dimensional hydrogen-bond-network to

393 stabilize GSH (Figure 4C, D). The G-site in AaGSTe2 was mainly formed by His53,

394 Ile55, Glu67, Ser68, and Arg112 with hydrogen bonds (Figure 4G, H). Comparing the

395 3D structure of AaGSTd3 and AaGSTe2 revealed that H2 in AaGSTe2 was closer to

396 β2 compared to AaGSTd3, and H8 was a few residues longer than in AaGSTd3.

397 The most favorable binding mode for 4,4'-DDT was in the H-site of AaGSTd3, with a

398 Gibbs free energy (ΔG) of -6.92 kcal/mol. The H-site of AaGSTd3 had an open

399 hydrophobic pocket adjacent to the G-site. The contributing residues for this putative

400 DDT-binding site included Ser6, Ile8, Ser9, Pro10, Thr31, Asn32, Ile33, Ile51, Ile108,

401 Ile111, and Val115 within 4Å distance, most of which were hydrophobic in nature,

402 while Ser6, Ser9, Thr31, and Asn32 were hydrophilic (Figure 5A, C).

403 The most favorable binding mode for 4,4'-DDT was in the H-site of AaGSTe2, with a

404 ΔG of -7.65 kcal/mol. The contributing residues for this putative DDT-binding included

405 Leu9, Leu11, Ser12, Pro13, Leu36, Leu37, Thr54, Ile55, Phe108, Met111, Arg112,

406 Phe115, Glu116, Leu119, Phe120, Leu207, and Phe210 within 4Å distance (Figure 5E,

407 G). Comparing the predicted DDT-binding sites of AaGSTd3 and AaGSTe2 revealed

408 that for AaGSTd3 H4 of the H-site is not bent, while for AaGSTe2, H4 of the H-site is

409 bent and forms a closed state pocket. Further, a closer distance between the 4,4'-DDT

410 molecule and GSH was observed for AaGSTe2. Last, the predicted DDT-binding

411 pocket for AaGSTe2 was surrounded by more residues - including residues from H8 -

412 forming a nearly closed state, while the pocket for AaGSTd3 was an open state,

413 although both of them were not predicted to have hydrogen bonds to stabilize 4,4'-DDT.

4. Discussion

GSTs confer resistance to insecticides by metabolizing - either via conjugation or dehydrochlorination - or sequestering pesticides. In addition, GSTs display peroxidase activity which can protect arthropods such as insects and mites against oxidative stress caused by insecticides and acaricides (Pavlidi et al., 2018). In mosquitoes, the epsilon class GST, GSTe2, has been frequently implicated in resistance against DDT. *GSTe2* was overexpressed in DDT-resistant *An. gambiae*, *An funestus* and *Ae. aegypti*, and the recombinant GSTe2s of these species could efficiently dehydrochlorinate DDT (Ding et al., 2003; Lumjuan et al., 2005; Ortelli et al., 2003; Riveron et al., 2014b). In addition, overexpression of *GSTe2* in transgenic mosquitoes conferred DDT resistance (Adolfi et al., 2019). Remarkably, a delta class GST gene, *GSTd3*, was also reported to be overexpressed in DDT/pyrethroid resistant *An. arabiensis*, *An. gambiae*, *An. coluzzii* and *An. funestus* populations (see Figure1/Table S1 for overview and references). Notably, overexpression of *GSTd3* occurs more frequently than *GSTe2* overexpression in DDT resistant anopheline populations (37 vs 30, Figure 1, Table S1), suggesting that *GSTd3* might be used as a resistance marker. However, in contrast to GSTe2, GSTd3 metabolism of DDT has not yet been investigated, or at least reported, and therefore we compare in this study the AaGSTd3 metabolism of DDT with that of AaGSTe2.

Both CDNB-conjugating and glutathione peroxidase activity was observed for AaGSTe2 and AaGSTd3. AaGSTe2 exhibited a significantly higher activity towards CDNB and showed higher glutathione peroxidase activity compared to AaGSTd3. Previously characterized AgGSTe2 CDNB-conjugating activity (12.5 μmol/mg/min) was found to be more than two-fold lower, but with similar kinetic parameters, compared to AaGSTe2. In contrast, glutathione peroxidase activity was not detected for AgGSTe2 in previous reports (Lumjuan et al., 2005; Ortelli et al., 2003). DDTase activity was also observed for both AaGSTe2 and AaGSTd3, with AaGSTd3 DDTase activity being slightly lower compared to previously characterized isoforms of *An. gambiae* GSTd1 (AgGSTd1-5 and AgGSTd1-6) but more than 80-fold lower than *An. dirus* GSTd5 and *A. sinensis* GSTd2 (Che-Mendoza et al., 2009; Ranson et al., 1998; Ranson et al., 1997; Tao et al., 2022; Udomsinprasert et al., 2005). However, caution is needed when comparing studies, as experimental conditions can significantly differ (e.g. 2 hour incubation assay at 28°C or 30°C and DDE detection with HPLC, compared to 6 hour incubation at 30°C and DDE detection with GC-ECD in this study) (Prapanthadara et al., 1993; Ranson et al., 1997; Tao et al., 2022). AaGSTe2, on the other hand, completely degraded DDT and DDE in the presence of GSH, while without GSH AaGSTe2 DDTase activity was almost four times higher than DDTase activity of

451 AaGSTd3 with GSH. Of important note, the DDTase activity of AaGSTe2 without
452 GSH was about 1000-fold lower than the previously reported DDTase activity of
453 AgGSTe2 with GSH (Ortelli et al., 2003). Complete degradation of DDE by AaGSTe2
454 has not yet been reported before, but might, as mentioned above, be due to different
455 reaction conditions. It could be that, when GSTe2 is incubated with DDT for a longer
456 period, AaGSTe2 reacts with DDE to form more water-soluble substrates (GS-DDE)
457 or even degrades DDE beyond DDD and, consequently, DDE can no longer be
458 extracted using organic solvents and detected by GC-ECD.

459 Molecular modeling showed that AaGSTd3 has a positive DDT-binding capability. The
460 most favorable binding mode for 4,4'-DDT was in the H-site of AaGSTd3 which had
461 an open hydrophobic pocket adjacent to the G-site, suggesting appropriate shape and
462 location of this pocket for DDT-binding capability. Surprisingly, a highly conserved G-
463 site residue in delta GSTs (Ser9) is missing in our docking model, which is in line with
464 DmGSTd2 and AdGSTd4-4 (Gonzalez et al., 2018; Vararattanavech and Ketterman,
465 2007). It could also imply that AaGSTd3 needs further formational change. Our
466 prediction of the AaGSTe2 protein structure and DDT docking was largely in line with
467 the findings of Wang et al. for AgGSTe2 (2008). Docking of DDT revealed that
468 AaGSTe2 has the same V-shaped DDT-binding pocket as AfGSTe2 and AgGSTe2, but
469 with the angle/shape of docked DDT differing between *Anopheles* GSTs, which could
470 be due to the protein sequence differences between *Anopheles* GSTe2s or different
471 docking software (Riveron et al., 2014b; Wang et al., 2008). Previous studies also
472 showed that the better performance of GSTe2 could be caused by a larger entry site for
473 DDT, a more efficient hydrogen bond network to stabilize GSH, and a better-sealed
474 hydrophobic DDT pocket (Low et al., 2010; Wang et al., 2008). Indeed, by comparing
475 the predicted DDT-binding sites of AaGSTd3 and AaGSTe2, it was found that H4 of
476 the H-site of AaGSTd3 is different from AaGSTe2, with H4 being bent and forming a
477 closed state pocket in *Anopheles* GSTe2 (Riveron et al., 2014b). In addition, the
478 predicted DDT-binding pocket for AaGSTe2 also comprised more residues compared
479 to AaGSTd3, forming a nearly closed state. Altogether, our molecular docking
480 experiments could explain higher DDT-detoxifying activity of AaGSTe2. In addition,
481 a closer position between chlorine atoms of DDT and the sulfur atom of glutathione
482 was also observed in AaGSTe2, which might facilitate the elimination of HCl from
483 DDT to form DDE (Low et al., 2010; Wongsantichon et al., 2012).

484 Although *GSTe2* is well known to confer DDT resistance, in some DDT/pyrethroid
485 field resistant populations from Africa, *GSTe2* is not always highly expressed nor is
486 the *GSTe2* L119F resistance mutation present, suggesting that additional mechanisms
487 are involved in DDT resistance in mosquitoes (Riveron et al., 2015; Simma et al., 2019;
488 Thomsen et al., 2014). Although AaGSTd3 metabolizes DDT to a lesser extent

compared to AaGSTe2 and has lower peroxidase activity, its consistent overexpression in DDT resistant anopheline populations suggests that it might have a significant role in DDT resistance. A possible explanation might be that GSTd3 rather sequesters than metabolizes DDT. In this light, AaGSTd3 does have a five-fold higher affinity for GSH compared to AaGSTe2 and previously it has been suggested that GSTs with high affinity for GSH evolved towards increased product binding at the expense of catalytic efficiency (Meyer, 1993). Alternatively, *GSTd3* might be co-regulated with other resistance genes, and make part of a more general stress response.

To conclude, both *GSTd3* and *GSTe2* of *An. arabiensis* were expressed and functionally characterized. CDNB-conjugating, DDTase and glutathione peroxidase activity of AaGSTd3 was lower compared to AaGSTe2. Protein modeling and DDT docking also suggested a better fit of DDT within the H-site AaGSTe2. This suggests that the contribution of AaGSTd3 towards DDT resistance in *Anopheles* mosquitoes is minor compared to that of AaGSTe2. However, the consistent overexpression of this gene in DDT resistant *Anopheles* mosquitoes, does suggest that *AaGSTd3* might have a significant role in resistance. Future experiments should focus on confirming the role of AaGSTd3 in DDT resistance, for example via genetically modified mosquitoes overexpressing *AaGSTd3* (as was done by Adolfi et al. for *AgGSTe2*), and investigate whether AaGSTd3 rather contributes to DDT resistance via sequestration instead of direct metabolism (Adolfi et al., 2019).

5. Author contributions

TVL and WD conceived and designed study, while PS provided resources. XPL performed experiments. XPL, TVL and WD analyzed data. XPL and ES wrote the manuscript, with input from WD and TVL. All authors read and approved the final manuscript.

6. Declaration of Competing Interest

The authors declare no competing of interest.

7. Acknowledgments

8. Funding

9. Figure legends

Figure 1. Expression levels of *GSTd3* and *GSTe2* in anopheline mosquito populations resistant to DDT

527 *GSTd3* and *GSTe2* expression levels [$\log_2$(fold change (FC)] derived from previously published
528 RNAseq studies with DDT resistant populations of *An. arabiensis*, *An. coluzzi, An gambiae s.s.*,
529 *An. gambiae* s.l. and *An. funestus*. A horizontal line indicates a $\log_2$FC of 1. An asterisk
530 indicates that the L119F resistance mutation was reported for GSTe2 (Riveron et al., 2017).
531 Details for each differential expression analysis can be found in Table S1.

Figure 2. DDT Metabolic activity assays with AaGSTe2 and AaGSTd3

533 (A) Concentration of DDT and its metabolite DDE at different time points in a reaction mix
534 including AaGSTd3, GSH, and DDT. (B) Concentration of DDT and its metabolite DDE at
535 different time points in a reaction mix system including AaGSTe2, GSH, and DDT. (C)
536 Concentration of DDT in a reaction mix with only AaGSTd3 and DDT. (D) Concentration of
537 DDT and its metabolite DDE in a reaction mix with only AaGSTe2 and DDT. (E) DDTase
538 activity of AaGSTd3 with (grey bars) or without GSH (black bars). (F) DDTase activity for
539 AaGSTe2 with (grey bars) or without GSH (black bars). A low or no DDTase activity was
540 shown for AaGSTe2 (grey bars) as only little DDE could be detected at 6h while at other time-
541 points DDT could not be detected. An asterisk indicates the treatment group at 6h is
542 significantly different from the control group at 6h (detailed information can be found in Figure
543 S4). Different letters a, b, c, d (or A, B, C, D) indicate statistically significant differences
544 between groups (one-way ANOVA, $P < 0.05$).

Figure 3. Multiple sequence alignment of *An. arabiensis* delta and epsilon class GSTs with those of insects

547 GST protein sequences were aligned using BioEdit v. 7.2.5 (Hall, 1999). BmGSTD (3VK9),
548 NlGSTD (3WYW), LmGSTD1(AEB91971), DmGSTD1(3EIN), AfGSTE2 (3ZML),
549 AgGSTD1-6 (1PN9), and AdGSTD4-4 (3F63) were used in this study, which can be accessed
550 at the NCBI (*L. migratoria*) or the RCSB Protein Data Bank (PDB accessions, other insects).
551 Identical and highly similar residues are shaded black and grey, respectively. The positions of
552 β sheets (β1-β4) and α-helices (H1-H8) in the AaGSTd3 protein sequence were derived from
553 the AaGSTd3 3D-model predicted by the Swiss-model server and are shown on top of the
554 alignment. The predicted GSH-binding pocket is indicated with an asterisk. The predicted
555 DDT-binding pockets are indicated with black squares. Bm: *Bombyx mori*; Nl: *Nilaparvata*

556 *lugens*; Lm: *Locusta migratoria*; Dm: *Drosophila melanogaster*; Af: *Anopheles funestus*; Ag:

557 *Anopheles gambiae*; Ad: *Anopheles duris*.

Figure 4. Structural features of AaGSTd3 and AaGSTe2 protein model

559 (A) Ribbon representation of the AaGSTd3 monomer. The N-terminal domain is shown in

560 purple, the C-terminal domain is shown in blue. (B) Ribbon representation of the AaGSTd3

561 homodimer. (C) Predicted residues that may contribute in the interaction of the GSH-binding

562 pockets in AaGSTd3. Hydrogen bonds are shown in red. (D) Predicted surface representation

563 of GSH binding in the AaGSTd3 protein model. (E) Ribbon representation of the AaGSTe2

564 monomer. The N-terminal domain is shown in purple while the C-terminal domain is shown in

565 blue. (F) Ribbon representation of the AaGSTe2 homodimer. (G) Predicted residues that may

566 contribute in the interaction of the GSH-binding pockets in AaGSTe2. Hydrogen bonds are

567 shown in red. (H) Predicted surface representation of GSH binding in the AaGSTe2 protein

568 model.

Figure 5. Predicted interactions between AaGSTd3 or AaGSTe2 residues and 4,4'-DDT

570 (A) Predicted residues that may contribute to the interaction of AaGSTd3 with 4,4'-DDT. (B)

571 Predicted surface representation of the DDT-binding pockets of AaGSTd3. (C) Predicted

572 residues that may contribute in the interaction of AaGSTd3 with a GSH and a DDT molecule.

573 (D) Predicted surface representation of the DDT-binding pockets in AaGSTd3. The bound GSH

574 molecule is also represented. Hydrogen bonds are shown in red. (E) Predicted residues that may

575 contribute to the interaction of AaGSTe2 with 4,4'-DDT. (F) Predicted surface representation

576 of the DDT-binding pockets of AaGSTe2. (G) Predicted residues that may contribute to the

577 interaction of AaGSTe2 with a GSH and a DDT molecule. (H) Predicted surface representation

578 of the DDT-binding pockets in AaGSTe2. The bound GSH molecule is also depicted. Hydrogen

579 bonds are shown in red.

10. Supplementary figure legends

Figure S1. Relative expression levels of *GSTd3* in DDT resistant populations of *An.*

582 **arabiensis**

583 Relative expression levels (fold change) of the *GSTd3* gene in highly DDT resistant *Anopheles*

584 *arabiensis* populations ASN, CHW and TOL compared to a susceptible population SEK as

585 assessed by RT-qPCR. An asterisk indicates a significant difference from 1 based on an

586 independent t test ($P < 0.05$).

Figure S2. Multiple sequence alignment of *An. arabiensis* and *An. gambiae GSTe2*

588 Alignment between *AaGSTe2* protein sequence of the TOL population, the AaGSTe2 protein

589 sequence (VectorBase ID: AARA008732) of the *An. arabiensis* reference strain (Dongola), and

590 the AgGSTe2 protein sequence (VectorBase ID: AGAP009194) of the *An. gambiae* reference
591 (PEST) strain. A square indicates previously reported resistance mutations (I114T, L119F) for
592 GSTe2, but these mutations were not found in the TOL population (Mitchell et al., 2014;
593 Riveron et al., 2014b). BioEdit v. 7.2.5 (Hall, 1999) was used for aligning sequences.

Figure S3. SDS-PAGE and Western blot of purified fractions of recombinantly expressed GST protein

596 SDS-PAGE (A) and Western blot (B) showing the expression of the AaGSTe2 and AaGSTd3
597 protein. Lane 1: molecular weight marker (Precision Plus Protein™ All Blue Prestained Protein
598 Standard). Lane 2: purified His-tagged AaGSTd3. Lane 3: purified His-tagged AaGSTe2. Lane
599 4: molecular weight marker (Precision Plus Protein™ Unstained Protein Standard).

Figure S4. DDT Metabolic activity assays with AaGSTe2 and AaGSTd3

601 DDT metabolic activity assays with AaGSTd3 were performed at 6h (A), 12h (B), 24h (C), and
602 36h (D). DDT metabolic activity assays with AaGSTe2 were performed at 6h (E), 12h (F), 24h
603 (G), and 36h (H). DDT, a reaction system including DDT only; DDE, a reaction system
604 including DDE only; Control, a reaction system including boiled GST, DDT and GSH; Without
605 GSH, a reaction system including GST and DDT; GSH, a reaction system including GST, DDT
606 and GSH. An asterisk indicates a significant difference from the control group at each time
607 point.

11. References

609 Abel, E. L., Bammler, T. K., and Eaton, D. L., 2004 **Biotransformation of methyl**
610   **parathion by glutathione S-transferases**. *Toxicol. Sci.,* 79, 224-232,
611   https://doi.org/10.1093/toxsci/kfh118.
612 Adolfi, A., Poulton, B., Anthousi, A., Macilwee, S., Ranson, H., and Lycett, G. J., 2019
613   **Functional genetic validation of key genes conferring insecticide resistance in the**
614   **major African malaria vector,** *Anopheles gambiae*. *Proc. Natl. Acad. Sci. U. S. A.,*
615   116, 25764-25772, https://doi.org/10.1073/pnas.1914633116.
616 Alemayehu, E., Asale, A., Eba, K., Getahun, K., Tushune, K., Bryon, A., Morou, E., Vontas,
617   J., Van Leeuwen, T., and Duchateau, L., 2017 **Mapping insecticide resistance and**
618   **characterization of resistance mechanisms in** *Anopheles arabiensis* **(Diptera:**
619   **Culicidae) in Ethiopia**. *Parasites Vectors,* 10, 1-11, https://doi.org/10.1186/s13071-
620   017-2342-y.
621 Antonio-Nkondjio, C., Sonhafouo-Chiana, N., Ngadjeu, C., Doumbe-Belisse, P., Talipouo,
622   A., Djamouko-Djonkam, L., Kopya, E., Bamou, R., Awono-Ambene, P., and Wondji,
623   C. S., 2017 **Review of the evolution of insecticide resistance in main malaria**
624   **vectors in Cameroon from 1990 to 2017**. *Parasites Vectors,* 10, 1-14,
625   https://doi.org/10.1186/s13071-017-2417-9.

626 Ayres, C., Müller, P., Dyer, N., Wilding, C., Rigden, D., and Donnelly, M., 2011
627   **Comparative genomics of the *anopheline* glutathione S-transferase epsilon**
628   **cluster**. *PLoS One,* 6, e29237, https://doi.org/10.1371/journal.pone.0029237.
629 Bradford, M. M., 1976 **A rapid and sensitive method for the quantitation of microgram**
630   **quantities of protein utilizing the principle of protein-dye binding**. *Anal.*
631   *Biochem.,* 72, 248-254, https://doi.org/10.1016/0003-2697(76)90527-3.
632 Brooks, B. R., Bruccoleri, R. E., Olafson, B. D., States, D. J., Swaminathan, S., and Karplus,
633   M., 1983 **CHARMM: a program for macromolecular energy, minimization, and**
634   **dynamics calculations**. *J. Comput. Chem.,* 4, 187-217,
635   https://doi.org/10.1002/jcc.540040211.
636 Che-Mendoza, A., Penilla, R. P., and Rodríguez, D. A., 2009 **Insecticide resistance and**
637   **glutathione S-transferases in mosquitoes: a review**. *Afr. J. Biotechnol.,* 8.
638 Clark, A. G., and Shamaan, N. A., 1984 **Evidence that DDT-dehydrochlorinase from the**
639   **house fly is a glutathione S-transferase**. *Pestic. Biochem. Physiol.,* 22, 249-261,
640   https://doi.org/10.1016/0048-3575(84)90018-X.
641 Clark, A. G., Shamaan, N. A., Sinclair, M. D., and Dauterman, W. C., 1986 **Insecticide**
642   **metabolism by multiple glutathione S-transferases in two strains of the house fly,**
643   ***Musca domestica* (L)**. *Pestic. Biochem. Physiol.,* 25, 169-175,
644   https://doi.org/10.1016/0048-3575(86)90044-1.
645 DeLano, W. L., 2002 **The PyMOL molecular graphics system**. *http://www.pymol.org*.
646 Dhiman, S., 2019 **Are malaria elimination efforts on right track? An analysis of gains**
647   **achieved and challenges ahead**. *Infect. Dis. Poverty,* 8, 1-19,
648   https://doi.org/10.1186/s40249-019-0524-x.
649 Ding, Y., Ortelli, F., Rossiter, L. C., Hemingway, J., and Ranson, H., 2003 **The *Anopheles***
650   ***gambiae* glutathione transferase supergene family: annotation, phylogeny and**
651   **expression profiles**. *BMC Genom.,* 4, 1-16, https://doi.org/10.1186/1471-2164-4-35.
652 Djouaka, R., Irving, H., Tukur, Z., and Wondji, C. S., 2011 **Exploring mechanisms of**
653   **multiple insecticide resistance in a population of the malaria vector *Anopheles***
654   ***funestus* in Benin**. *PLoS One,* 6, e27760,
655   https://doi.org/10.1371/journal.pone.0027760.
656 Enayati, A. A., Ranson, H., and Hemingway, J., 2005 **Insect glutathione transferases and**
657   **insecticide resistance**. *Insect Mol. Biol.,* 14, 3-8, https://doi.org/10.1111/j.1365-
658   2583.2004.00529.x.
659 Feyereisen, R., Dermauw, W., and Van Leeuwen, T., 2015 **Genotype to phenotype, the**
660   **molecular and physiological dimensions of resistance in arthropods**. *Pestic.*
661   *Biochem. Physiol.,* 121, 61-77, https://doi.org/10.1016/j.pestbp.2015.01.004.
662 Fossog Tene, B., Poupardin, R., Costantini, C., Awono-Ambene, P., Wondji, C. S., Ranson,
663   H., and Antonio-Nkondjio, C., 2013 **Resistance to DDT in an urban setting:**
664   **common mechanisms implicated in both M and S forms of *Anopheles gambiae* in**
665   **the city of Yaoundé Cameroon**. *PLoS One,* 8, e61408,
666   https://doi.org/10.1371/journal.pone.0061408.
667 Gonzalez, D., Fraichard, S., Grassein, P., Delarue, P., Senet, P., Nicolaï, A., Chavanne, E.,
668   Mucher, E., Artur, Y., and Ferveur, J.-F., 2018 **Characterization of a *Drosophila***

669 **glutathione transferase involved in isothiocyanate detoxification**. *Insect Biochem.*
670 *Mol. Biol.,* 95, 33-43, https://doi.org/10.1016/j.ibmb.2018.03.004.
671 Grant, D. F., Dietze, E. C., and Hammock, B. D., 1991 **Glutathione S-transferase isozymes**
672 **in *Aedes aegypti*: purification, characterization, and isozyme-specific regulation**.
673 *Insect Biochem.,* 21, 421-433, https://doi.org/10.1016/0020-1790(91)90009-4.
674 Haberthür, U., and Caflisch, A., 2008 **FACTS: Fast analytical continuum treatment of**
675 **solvation**. *J. Comput. Chem.,* 29, 701-715, https://doi.org/10.1002/jcc.20832.
676 Habig, W. H., Pabst, M. J., and Jakoby, W. B., 1974 **Glutathione S-transferases: the first**
677 **enzymatic step in mercapturic acid formation**. *J. Biol. Chem.,* 249, 7130-7139,
678 https://doi.org/10.1016/S0021-9258(19)42083-8.
679 Hall, T. A., 1999 **BioEdit: a user-friendly biological sequence alignment editor and**
680 **analysis program for Windows 95/98/NT**. *Nucleic Acids Symp. Ser.,* 41, 95-98.
681 Hancock, P. A., Hendriks, C. J., Tangena, J.-A., Gibson, H., Hemingway, J., Coleman, M.,
682 Gething, P. W., Cameron, E., Bhatt, S., and Moyes, C. L., 2020 **Mapping trends in**
683 **insecticide resistance phenotypes in African malaria vectors**. *PLoS Biol.,* 18,
684 e3000633, https://doi.org/10.1371/journal.pbio.3000633.
685 Hayes, J. D., and Wolf, C. R., 1988 **Role of glutathione transferase in drug resistance**. *In*
686 "Glutathione conjugation: mechanisms and biological significance", pp. 3150-355.
687 Academic Press, London, UK,
688 Hemingway, J., Hawkes, N. J., McCarroll, L., and Ranson, H., 2004 **The molecular basis of**
689 **insecticide resistance in mosquitoes**. *Insect Biochem. Mol. Biol.,* 34, 653-665,
690 https://doi.org/10.1016/j.ibmb.2004.03.018.
691 Hemingway, J., and Ranson, H., 2000 **Insecticide resistance in insect vectors of human**
692 **disease**. *Annu. Rev. Entomol.,* 45, 371-391,
693 https://doi.org/10.1146/annurev.ento.45.1.371.
694 Ibrahim, S. S., Muhammad, A., Hearn, J., Weedall, G. D., Nagi, S. C., Mukhtar, M. M.,
695 Fadel, A. N., Mugenzi, L. M., Patterson, E. I., and Irving, H., 2022 **Molecular**
696 **drivers of insecticide resistance in the Sahelo-Sudanian populations of a major**
697 **malaria vector**. *bioRxiv*, https://doi.org/10.1101/2022.03.21.485146.
698 Ingham, V., Wagstaff, S., and Ranson, H., 2018 **Transcriptomic meta-signatures identified**
699 **in *Anopheles gambiae* populations reveal previously undetected insecticide**
700 **resistance mechanisms**. *Nat. Commun.,* 9, 1-11, https://doi.org/10.1038/s41467-018-
701 07615-x.
702 Isaacs, A. T., Mawejje, H. D., Tomlinson, S., Rigden, D. J., and Donnelly, M. J., 2018
703 **Genome-wide transcriptional analyses in *Anopheles* mosquitoes reveal an**
704 **unexpected association between salivary gland gene expression and insecticide**
705 **resistance**. *BMC Genom.,* 19, 1-12, https://doi.org/10.1186/s12864-018-4605-1.
706 Jones, C. M., Toé, H. K., Sanou, A., Namountougou, M., Hughes, A., Diabaté, A., Dabiré, R.,
707 Simard, F., and Ranson, H., 2012 **Additional selection for insecticide resistance in**
708 **urban malaria vectors: DDT resistance in *Anopheles arabiensis* from Bobo-**
709 **Dioulasso, Burkina Faso**. *PLoS One*, e45995,
710 https://doi.org/10.1371/journal.pone.0045995.
711 Kleinschmidt, I., Bradley, J., Knox, T. B., Mnzava, A. P., Kafy, H. T., Mbogo, C., Ismail, B.
712 A., Bigoga, J. D., Adechoubou, A., and Raghavendra, K., 2018 **Implications of**

insecticide resistance for malaria vector control with long-lasting insecticidal nets: a WHO-coordinated, prospective, international, observational cohort study. *Lancet Infect. Dis.,* 18, 640-649, https://doi.org/10.1016/S1473-3099(18)30172-5.

Kostaropoulos, I., Papadopoulos, A. I., Metaxakis, A., Boukouvala, E., and Papadopoulou-Mourkidou, E., 2001 **Glutathione S–transferase in the defence against pyrethroids in insects**. *Insect Biochem. Mol. Biol.,* 31, 313-319, https://doi.org/10.1016/S0965-1748(00)00123-5.

Kouamo, M. F., Ibrahim, S. S., Hearn, J., Riveron, J. M., Kusimo, M., Tchouakui, M., Ebai, T., Tchapga, W., Wondji, M. J., and Irving, H., 2021 **Genome-wide transcriptional analysis and functional validation linked a cluster of epsilon glutathione S-transferases with insecticide resistance in the major malaria vector *Anopheles funestus* across Africa**. *Genes,* 12, 561, https://doi.org/10.3390/genes12040561.

Lawson, D., Arensburger, P., Atkinson, P., Besansky, N. J., Bruggner, R. V., Butler, R., Campbell, K. S., Christophides, G. K., Christley, S., and Dialynas, E., 2009 **VectorBase: a data resource for invertebrate vector genomics**. *Nucleic Acids Res.,* 37, D583-D587, https://doi.org/10.1093/nar/gkn857.

Liu, N., 2015 **Insecticide resistance in mosquitoes: impact, mechanisms, and research directions**. *Annu. Rev. Entomol.,* 60, 537-59, https://doi.org/10.1146/annurev-ento-010814-020828.

Low, W. Y., Feil, S. C., Ng, H. L., Gorman, M. A., Morton, C. J., Pyke, J., McConville, M. J., Bieri, M., Mok, Y.-F., and Robin, C., 2010 **Recognition and detoxification of the insecticide DDT by *Drosophila melanogaster* glutathione S-transferase D1**. *J. Mol. Biol.,* 399, 358-366, https://doi.org/10.1016/j.jmb.2010.04.020.

Lumjuan, N., McCarroll, L., Prapanthadara, L.-a., Hemingway, J., and Ranson, H., 2005 **Elevated activity of an Epsilon class glutathione transferase confers DDT resistance in the dengue vector, *Aedes aegypti***. *Insect Biochem. Mol. Biol.,* 35, 861-871, https://doi.org/10.1016/j.ibmb.2005.03.008.

Lumjuan, N., Rajatileka, S., Changsom, D., Wicheer, J., Leelapat, P., Prapanthadara, L.-a., Somboon, P., Lycett, G., and Ranson, H., 2011 **The role of the *Aedes aegypti* Epsilon glutathione transferases in conferring resistance to DDT and pyrethroid insecticides**. *Insect Biochem. Mol. Biol.,* 41, 203-209, https://doi.org/10.1016/j.ibmb.2010.12.005.

Lumjuan, N., Stevenson, B. J., Prapanthadara, L.-a., Somboon, P., Brophy, P. M., Loftus, B. J., Severson, D. W., and Ranson, H., 2007 **The *Aedes aegypti* glutathione transferase family**. *Insect Biochem. Mol. Biol.,* 37, 1026-1035, https://doi.org/10.1016/j.ibmb.2007.05.018.

Mannervik, B., Helena Danielson, U., and Ketterer, B., 1988 **Glutathione transferases—structure and catalytic activit**. *Crit. Rev. Biochem.,* 23, 283-337, https://doi.org/10.3109/10409238809088226.

Matiya, D. J., Philbert, A. B., Kidima, W., and Matowo, J. J., 2019 **Dynamics and monitoring of insecticide resistance in malaria vectors across mainland Tanzania from 1997 to 2017: a systematic review**. *Malar. J.,* 18, 1-16, https://doi.org/10.1186/s12936-019-2738-6.

Mekonen, S., Lachat, C., Ambelu, A., Steurbaut, W., Kolsteren, P., Jacxsens, L., Wondafrash, M., Houbraken, M., and Spanoghe, P., 2015 **Risk of DDT residue in maize consumed by infants as complementary diet in southwest Ethiopia**. *Sci. Total Environ.,* 511, 454-460, https://doi.org/10.1016/j.scitotenv.2014.12.087.

Messenger, L. A., Impoinvil, L. M., Derilus, D., Yewhalaw, D., Irish, S., and Lenhart, A., 2021 **A whole transcriptomic approach provides novel insights into the molecular basis of organophosphate and pyrethroid resistance in *Anopheles arabiensis* from Ethiopia**. *Insect Biochem. Mol. Biol.,* 139, 103655, https://doi.org/10.1016/j.ibmb.2021.103655.

Meyer, D. J., 1993 **Significance of an unusually low *Km* for glutathione in glutathione transferases of the α μ and π classes**. *Xenobiotica,* 23, 823-834, https://doi.org/10.3109/00498259309059411.

Mitchell, S. N., Rigden, D. J., Dowd, A. J., Lu, F., Wilding, C. S., Weetman, D., Dadzie, S., Jenkins, A. M., Regna, K., and Boko, P., 2014 **Metabolic and target-site mechanisms combine to confer strong DDT resistance in *Anopheles gambiae***. *PLoS One,* 9, e92662, https://doi.org/10.1371/journal.pone.0092662.

Müller, P., Warr, E., Stevenson, B. J., Pignatelli, P. M., Morgan, J. C., Steven, A., Yawson, A. E., Mitchell, S. N., Ranson, H., and Hemingway, J., 2008 **Field-caught permethrin-resistant *Anopheles gambiae* overexpress CYP6P3, a P450 that metabolises pyrethroids**. *PLoS Genet.,* 4, e1000286, https://doi.org/10.1371/journal.pgen.1000286.

Nardini, L., Christian, R. N., Coetzer, N., Ranson, H., Coetzee, M., and Koekemoer, L. L., 2012 **Detoxification enzymes associated with insecticide resistance in laboratory strains of *Anopheles arabiensis* of different geographic origin**. *Parasites Vectors,* 5, 1-12, https://doi.org/10.1186/1756-3305-5-113.

Ortelli, F., Rossiter, L. C., Vontas, J., Ranson, H., and Hemingway, J., 2003 **Heterologous expression of four glutathione transferase genes genetically linked to a major insecticide-resistance locus from the malaria vector *Anopheles gambiae***. *Biochem. J.,* 373, 957-963, https://doi.org/10.1042/bj20030169.

Pavlidi, N., Vontas, J., and Van Leeuwen, T., 2018 **The role of glutathione S-transferases (GSTs) in insecticide resistance in crop pests and disease vectors**. *Curr. Opin. Insect Sci.,* 27, 97-102, https://doi.org/10.1016/j.cois.2018.04.007.

Pickett, C. B., and Lu, A. Y., 1989 **Glutathione S-transferases: gene structure, regulation, and biological function**. *Annu. Rev. Biochem.,* 58, 743-764, https://doi.org/10.1146/annurev.bi.58.070189.003523.

Polson, K. A., Brogdon, W. G., Rawlins, S. C., and Chadee, D. D., 2011 **Characterization of insecticide resistance in Trinidadian strains of *Aedes aegypti* mosquitoes**. *Acta Tropica,* 117, 31-38, https://doi.org/10.1016/j.actatropica.2010.09.005.

Prapanthadara, L.-a., Hemingway, J., and Ketterman, A. J., 1995 **DDT-resistance in *Anopheles gambiae* (Diptera: Culicidae) from Zanzibar, Tanzania, based on increased DDT-dehydrochlorinase activity of glutathione S-transferases**. *Bull. Entomol. Res.,* 85, 267-274, https://doi.org/10.1017/S0007485300034350.

Prapanthadara, L.-A., Koottathep, S., Promtet, N., Hemingway, J., and Ketterman, A. J., 1996 **Purification and characterization of a major glutathione S-transferase from the**

mosquito *Anopheles dirus* **(species B)**. *Insect Biochem. Mol. Biol.,* 26, 277-285, https://doi.org/10.1016/0965-1748(95)00090-9.

Prapanthadara, L., Promtet, N., Koottathep, S., Somboon, P., and Ketterman, A. J., 2000 **Isoenzymes of glutathione S-transferase from the mosquito *Anopheles dirus* species B: the purification, partial characterization and interaction with various insecticides**. *Insect Biochem. Mol. Biol.,* 30, 395-403, https://doi.org/10.1016/S0965-1748(00)00013-8.

Prapanthadara, L. A., Hemingway, J., and Ketterman, A. J., 1993 **Partial purification and characterization of glutathione S-transferases involved in DDT resistance from the mosquito *Anopheles gambiae***. *Pestic. Biochem. Physiol.,* 47, 119-133, https://doi.org/10.1006/pest.1993.1070.

Ranson, H., Claudianos, C., Ortelli, F., Abgrall, C., Hemingway, J., Sharakhova, M. V., Unger, M. F., Collins, F. H., and Feyereisen, R., 2002 **Evolution of supergene families associated with insecticide resistance**. *Science,* 298, 179-181, https://doi.org/10.1126/science.1076781.

Ranson, H., Collins, F., and Hemingway, J., 1998 **The role of alternative mRNA splicing in generating heterogeneity within the *Anopheles gambiae* class I glutathione S-transferase family**. *Proc. Natl. Acad. Sci. U. S. A.,* 95, 14284-14289, https://doi.org/10.1073/pnas.95.24.14284.

Ranson, H., Prapanthadara, L.-a., and Hemingway, J., 1997 **Cloning and characterization of two glutathione S-transferases from a DDT-resistant strain of *Anopheles gambiae***. *Biochem. J.,* 324, 97-102, https://doi.org/10.1042/bj3240097.

Ranson, H., Rossiter, L., Ortelli, F., Jensen, B., Wang, X., Roth, C. W., Collins, F. H., and Hemingway, J., 2001 **Identification of a novel class of insect glutathione S-transferases involved in resistance to DDT in the malaria vector *Anopheles gambiae***. *Biochem. J.,* 359, 295-304, https://doi.org/10.1042/bj3590295.

Riveron, J. M., Chiumia, M., Menze, B. D., Barnes, K. G., Irving, H., Ibrahim, S. S., Weedall, G. D., Mzilahowa, T., and Wondji, C. S., 2015 **Rise of multiple insecticide resistance in *Anopheles funestus* in Malawi: a major concern for malaria vector control**. *Malar. J.,* 14, 1-9, https://doi.org/10.1186/s12936-015-0877-y.

Riveron, J. M., Ibrahim, S. S., Chanda, E., Mzilahowa, T., Cuamba, N., Irving, H., Barnes, K. G., Ndula, M., and Wondji, C. S., 2014a **The highly polymorphic *CYP6M7* cytochrome P450 gene partners with the directionally selected *CYP6P9a* and *CYP6P9b* genes to expand the pyrethroid resistance front in the malaria vector *Anopheles funestus* in Africa**. *BMC Genom.,* 15, 1-19, https://doi.org/10.1186/1471-2164-15-817.

Riveron, J. M., Ibrahim, S. S., Mulamba, C., Djouaka, R., Irving, H., Wondji, M. J., Ishak, I. H., and Wondji, C. S., 2017 **Genome-wide transcription and functional analyses reveal heterogeneous molecular mechanisms driving pyrethroids resistance in the major malaria vector *Anopheles funestus* across Africa**. *G3: Genes, Genomes, Genet.,* 7, 1819-1832, https://doi.org/10.1534/g3.117.040147.

Riveron, J. M., Yunta, C., Ibrahim, S. S., Djouaka, R., Irving, H., Menze, B. D., Ismail, H. M., Hemingway, J., Ranson, H., and Albert, A., 2014b **A single mutation in the *GSTe2* gene allows tracking of metabolically based insecticide resistance in a**

845 **major malaria vector**. *Genome Biol.,* 15, 1-20, https://doi.org/10.1186/gb-2014-15-
846 2-r27.

847 Samb, B., Konate, L., Irving, H., Riveron, J. M., Dia, I., Faye, O., and Wondji, C. S., 2016
848 **Investigating molecular basis of lambda-cyhalothrin resistance in an *Anopheles***
849 ***funestus* population from Senegal**. *Parasites Vectors,* 9, 1-10,
850 https://doi.org/10.1186/s13071-016-1735-7.

851 Samra, A. I., Kamita, S. G., Yao, H. W., Cornel, A. J., and Hammock, B. D., 2012 **Cloning**
852 **and characterization of two glutathione S-transferases from pyrethroid-resistant**
853 ***Culex pipiens***. *Pest Manage. Sci.,* 68, 764-772, https://doi.org/10.1002/ps.2324.

854 Sawicki, R., Singh, S. P., Mondal, A. K., Beneš, H., and Zimniak, P., 2003 **Cloning,**
855 **expression and biochemical characterization of one Epsilon-class (GST-3) and**
856 **ten Delta-class (GST-1) glutathione S-transferases from *Drosophila***
857 ***melanogaster*, and identification of additional nine members of the Epsilon class**.
858 *Biochem. J.,* 370, 661-669, https://doi.org/10.1042/bj20021287.

859 Silva, A. P. B., Santos, J. M. M., and Martins, A. J., 2014 **Mutations in the voltage-gated**
860 **sodium channel gene of anophelines and their association with resistance to**
861 **pyrethroids–a review**. *Parasites Vectors,* 7, 1-14, https://doi.org/10.1186/1756-
862 3305-7-450.

863 Simma, E. A., Dermauw, W., Balabanidou, V., Snoeck, S., Bryon, A., Clark, R. M.,
864 Yewhalaw, D., Vontas, J., Duchateau, L., and Van Leeuwen, T., 2019 **Genome-wide**
865 **gene expression profiling reveals that cuticle alterations and P450 detoxification**
866 **are associated with deltamethrin and DDT resistance in *Anopheles arabiensis***
867 **populations from Ethiopia**. *Pest Manage. Sci.,* 75, 1808-1818,
868 https://doi.org/10.1002/ps.5374.

869 Singh, S. P., Coronella, J. A., Beneš, H., Cochrane, B. J., and Zimniak, P., 2001 **Catalytic**
870 **function of *Drosophila melanogaster* glutathione S-transferase DmGSTS1-1**
871 **(GST-2) in conjugation of lipid peroxidation end products**. *Eur. J. Biochem.,* 268,
872 2912-2923, https://doi.org/10.1046/j.1432-1327.2001.02179.x.

873 Stevenson, B. J., Bibby, J., Pignatelli, P., Muangnoicharoen, S., O'Neill, P. M., Lian, L.-Y.,
874 Müller, P., Nikou, D., Steven, A., and Hemingway, J., 2011 **Cytochrome P450 6M2**
875 **from the malaria vector *Anopheles gambiae* metabolizes pyrethroids: sequential**
876 **metabolism of deltamethrin revealed**. *Insect Biochem. Mol. Biol.,* 41, 492-502,
877 https://doi.org/10.1016/j.ibmb.2011.02.003.

878 Strode, C., Wondji, C. S., David, J.-P., Hawkes, N. J., Lumjuan, N., Nelson, D. R., Drane, D.
879 R., Karunaratne, S. P., Hemingway, J., and Black IV, W. C., 2008 **Genomic analysis**
880 **of detoxification genes in the mosquito *Aedes aegypti***. *Insect Biochem. Mol. Biol.,*
881 38, 113-123, https://doi.org/10.1016/j.ibmb.2007.09.007.

882 Takken, W., and Lindsay, S., 2019 **Increased threat of urban malaria from *Anopheles***
883 ***stephensi* mosquitoes, Africa**. *Emerg. Infect. Dis.,* 25, 1431,
884 https://doi.org/10.3201/eid2507.190301.

885 Tao, F., Si, F. L., Hong, R., He, X., Li, X. Y., Qiao, L., He, Z. B., Yan, Z. T., He, S. L., and
886 Chen, B., 2022 **Glutathione S-transferase (GST) genes and their function**
887 **associated with pyrethroid resistance in the malaria vector *Anopheles sinensis***.
888 *Pest Manage. Sci.*, https://doi.org/10.1002/ps.7031.

Tchigossou, G., Djouaka, R., Akoton, R., Riveron, J. M., Irving, H., Atoyebi, S., Moutairou, K., Yessoufou, A., and Wondji, C. S., 2018 **Molecular basis of permethrin and DDT resistance in an *Anopheles funestus* population from Benin**. *Parasites Vectors,* 11, 1-13, https://doi.org/10.1186/s13071-018-3115-y.

Thomsen, E. K., Strode, C., Hemmings, K., Hughes, A. J., Chanda, E., Musapa, M., Kamuliwo, M., Phiri, F. N., Muzia, L., and Chanda, J., 2014 **Underpinning sustainable vector control through informed insecticide resistance management**. *PLoS One,* 9, e99822, https://doi.org/10.1371/journal.pone.0099822.

Toé, K. H., N'Falé, S., Dabiré, R. K., Ranson, H., and Jones, C. M., 2015 **The recent escalation in strength of pyrethroid resistance in *Anopheles coluzzi* in West Africa is linked to increased expression of multiple gene families**. *BMC Genom.,* 16, 1-11, https://doi.org/10.1186/s12864-015-1342-6.

Tu, C. P. D., and Akgül, B., 2005 ***Drosophila* glutathione S-transferases**. *Methods Enzymol.,* 401, 204-226, https://doi.org/10.1016/S0076-6879(05)01013-X.

Udomsinprasert, R., Pongjaroenkit, S., Wongsantichon, J., Oakley, A. J., Prapanthadara, L.-a., Wilce, M. C. J., and Ketterman, A. J., 2005 **Identification, characterization and structure of a new Delta class glutathione transferase isoenzyme**. *Biochem. J.,* 388, 763-771, https://doi.org/10.1042/BJ20042015.

Vararattanavech, A., and Ketterman, A. J., 2007 **A functionally conserved basic residue in glutathione transferases interacts with the glycine moiety of glutathione and is pivotal for enzyme catalysis**. *Biochem. J.,* 406, 247-256, https://doi.org/10.1042/BJ20070422.

Vontas, J. G., Small, G. J., and Hemingway, J., 2001 **Glutathione S-transferases as antioxidant defence agents confer pyrethroid resistance in *Nilaparvata lugens***. *Biochem. J.,* 357, 65-72, https://doi.org/10.1042/bj3570065.

Wang, Y., Qiu, L., Ranson, H., Lumjuan, N., Hemingway, J., Setzer, W. N., Meehan, E. J., and Chen, L., 2008 **Structure of an insect epsilon class glutathione S-transferase from the malaria vector *Anopheles gambiae* provides an explanation for the high DDT-detoxifying activity**. *J. Struct. Biol.,* 164, 228-235, https://doi.org/10.1016/j.jsb.2008.08.003.

WHO, 2022 "**World malaria report 2022**," World Health Organization,

Wiebe, A., Longbottom, J., Gleave, K., Shearer, F. M., Sinka, M. E., Massey, N. C., Cameron, E., Bhatt, S., Gething, P. W., and Hemingway, J., 2017 **Geographical distributions of African malaria vector sibling species and evidence for insecticide resistance**. *Malar. J.,* 16, 1-10, https://doi.org/10.1186/s12936-017-1734-y.

Wipf, N. C., Duchemin, W., Kouadio, F.-P. A., Fodjo, B. K., Sadia, C. G., Mouhamadou, C. S., Vavassori, L., Mäser, P., Mavridis, K., and Vontas, J., 2022 **Multi-insecticide resistant malaria vectors in the field remain susceptible to malathion, despite the presence of *Ace1* point mutations**. *PLoS Genet.,* 18, e1009963, https://doi.org/10.1371/journal.pgen.1009963.

Wongsantichon, J., Robinson, R. C., and Ketterman, A. J., 2012 **Structural evidence for conformational changes of delta class glutathione transferases after ligand**

932 **binding**. *Arch. Biochem. Biophys.,* 521, 77-83,
933 https://doi.org/10.1016/j.abb.2012.03.023.
934 Wongtrakul, J., Pongjaroenkit, S., Leelapat, P., Nachaiwieng, W., Prapanthadara, L.-A., and
935 Ketterman, A. J., 2014 **Expression and characterization of three new glutathione**
936 **transferases, an epsilon (AcGSTE2-2), omega (AcGSTO1-1), and theta**
937 **(AcGSTT1-1) from** *Anopheles cracens* **(Diptera: Culicidae), a major Thai**
938 **malaria vector**. *J. Med. Entomol.,* 47, 162-171,
939 https://doi.org/10.1093/jmedent/47.2.162.
940 Wybouw, N., Balabanidou, V., Ballhorn, D., Dermauw, W., Grbić, M., Vontas, J., and Van
941 Leeuwen, T., 2012 **A horizontally transferred cyanase gene in the spider mite**
942 *Tetranychus urticae* **is involved in cyanate metabolism and is differentially**
943 **expressed upon host plant change**. *Insect Biochem. Mol. Biol.,* 42, 881-889,
944 https://doi.org/10.1016/j.ibmb.2012.08.002.
945 Yang, Y., Cheng, J.-Z., Singhal, S. S., Saini, M., Pandya, U., Awasthi, S., and Awasthi, Y. C.,
946 2001 **Role of glutathione S-transferases in protection against lipid peroxidation:**
947 **overexpression of hGSTA2-2 in K562 cells protects against hydrogen peroxide-**
948 **induced apoptosis and inhibits JNK and caspase 3 activation**. *J. Biol. Chem.,* 276,
949 19220-19230, https://doi.org/10.1074/jbc.M100551200.
950 You, Y., Xie, M., Ren, N., Cheng, X., Li, J., Ma, X., Zou, M., Vasseur, L., Gurr, G. M., and
951 You, M., 2015 **Characterization and expression profiling of glutathione S-**
952 **transferases in the diamondback moth,** *Plutella xylostella* **(L.)**. *BMC Genom.,* 16,
953 1-13, https://doi.org/10.1186/s12864-015-1343-5.

954

955

956

957
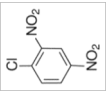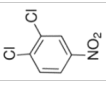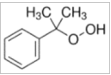
12. Tables

Table 1. Substrate specificities of AaGSTd3 and AaGSTe2 against the model substrates CDNB, DCNB, and CuOOH

Substrate	Structure	Specific activity (µmol/min/mg)	
		AaGSTd3	**AaGSTe2**
1-Chloro-2,4-dinitrobenzene (CDNB)		0.68 ± 0.09	33 ± 3*
1,2-Dichloro-4-nitrobenzene (DCNB)		n.d.	0.27 ± 0.02*
Cumene hydroperoxide (CuOOH)		0.55 ± 0.06	1.8 ± 0.2*

n.d: not detected (under assay conditions)

An asterisk indicates a significant difference from AaGSTd3 based on an independent t test ($P < 0.05$).

965 **Table2. Kinetic parameters of recombinant *Anopheles arabiensis* GSTs**

Kinetic parameter	AaGSTd3	AaGSTe2
V_{max}^{CDNB} (U/mg)	0.65 ± 0.02	24 ± 2*
V_{max}^{GSH} (U/mg)	0.72 ± 0.05	41 ± 2*
K_m^{CDNB} (mM)	1.3 ± 0.1	0.0093 ± 0.0008*
K_m^{GSH} (mM)	1.2 ± 0.1	6.8 ± 0.8*
k_{cat}^{CDNB} (s^{-1})	0.27 ± 0.01	10 ± 1*
k_{cat}^{GSH} (s^{-1})	0.30 ± 0.02	18 ± 1*
k_{cat}/K_m^{CDNB} (mM^{-1}s^{-1})	0.21	1100
k_{cat}/K_m^{GSH} (mM^{-1}s^{-1})	0.24	2.6

966 Three independent assays were performed and four technical replicates were used in each independent assay. Results show mean $\pm$ SE. One unit (U) is the
967 amount of enzyme that catalyzes the reaction of 1 μmol of substrate per minute at pH 6.5 and 30ºC. An asterisk indicates a significant difference from
968 AaGSTd3 based on an independent t test ($P < 0.05$).

969

970

971

972

13. Supplementary Tables

Table S1. Relative expression level of *GSTd3* and *GSTe2* in anopheline mosquito populations

Table S2. Primers used in this study

Table S3. Codon optimized sequence of *AaGSTd3* and *AaGSTe2* for expression in *Escherichia coli*

Table S4. CDS of *AaGSTe2* from reference (Dongola) and the resistant TOL population and CDS of *AgGSTe2* from reference (PEST) population.

979

AaGSTd3

AaGSTe2

980

Secondary structure labels (top): β1 H1 β2 H2

```
AaGSTd3    1   ---MDYYYSLISPPGQSAILVAKKLGITLNLKKTNIHDP-VERDALTKLN  46
AdGSTd4-4  1   ---MDFYYLPGSAPGRAVQMTAAAVGVELNLKLTNLMAGEHMKPEFLKLN  47
AgGSTd1-6  1   ---MDFYYLPGSAPGRAVQMTAAAVGVELNLKLTDLMKGEHMKPEFLKLN  47
DmGSTd1    1   --MVDFYYLPGSSPGRSVIMTAKAVGVELNLKKLNLQAGEHLKPEFLKIN  48
BmGSTd     1   -MTIDLYYVPGSAPGRAVLLTAKALNLNLNLKLVDLHHGEQLKPEYLKLN  49
LmGSTd1    1   MPSVDLYYVPGSAPGRAVQMVAKAVGVDLNLKLVNLMEGEQMKPEYLKMN  50
NlGSTd     1   -MPIDLYYVPGSAPGRNVLLAAKAVGVDLNLKLTDLKSGQHLTPEFIKLN  49
AfGSTe2    1   MTKLVLYTLHLSPPGRAVELTAKALGLELEQKNINLLAGDHLKPEFMKLN  50
AaGSTe2    1   MSKLVLYTLHLSPPGRAVELTAKALGLELEQKTINLLTGDHLKPEFLKLN  50
```

Secondary structure labels (bottom): β1 H1 β2 H2

Secondary structure labels (top): β3 β4 H3 linker

```
AaGSTd3    47  PQHTIPTLVDN-GHVVWESYAIVTYLVEVYGKDD-----TLYPKDPKVRS  90
AdGSTd4-4  48  PQHCIPTLVDEDGFVLWESRAIQIYLVEKYGAHDADLAERLYPSDPRRRA  97
AgGSTd1-6  48  PQHCIPTLVDN-GFALWESRAIQIYLAEKYGKDD-----KLYPKDPQKRA  91
DmGSTd1    49  PQHTIPTLVDN-GFALWESRAIQVYLVNKYAKGS-----SLYPKCPKKRA  92
BmGSTd     50  PQHTVPTLVDD-GLSIWESRAIITYLVNKYAKGS-----SLYPEDPKARA  93
LmGSTd1    51  PQHTVPTIDDN-GLYLWESRAIIGYLVEQYGKDD-----SLYPKEAKKRA  94
NlGSTd     50  PQHNVPTLDDN-GFVLNESRAIMTYLADQYGKDD-----SLYPKDPKKRA  93
AfGSTe2    51  PQHTIPVLDDD-GTIITESHAIMIYLVTKYGKDD-----TLYPKDPVQQA  94
AaGSTe2    51  PQHTIPVLDDN-GTIITESHAIMIYLVTKYGKDD-----SLYPKDPVKQA  94
```

Secondary structure labels (bottom): β3 β4 H3 linker

Secondary structure labels (top): H4 H5

```
AaGSTd3    91  VVNQRLFFDIGTLYKQIIDIIHLVVKKEQP---TDEQMEKLKKAMDLLEH  137
AdGSTd4-4  98  VVHQRLFFDVAVLYRFAEYYYPQIFGQKVPVGDPGRLRSMEQALEFLNT  147
AgGSTd1-6  92  VVNQRLYFDMGTLYQRFADYHYPQIFAKQP--ANPENEKKMKDAVGFLNT  139
DmGSTd1    93  VINQRLYFDMGTLYQSFANYYYPQVFAKAP--ADPEAFKKIEAAFEFLNT  140
BmGSTd     94  LVDQRLYFDIGTLYQRFSDYFYPQVFAGAP--ADKAKNEKVQEALQLLDK  141
LmGSTd1    95  LVNQRMYFDIGTLYARFADYYYPVMFGGAS--YDPEKLKKLEEAYEFLNK  142
NlGSTd     94  KVNQRLYFDMGTLYQSFGDAYYPHMFGGAP--LDEDKKKKLGDALVFLDG  141
AfGSTe2    95  RVNAALHFESGVLFARMRFIFERILFYGKSD-IPEDRIEYVQKSYRLLED  143
AaGSTe2    95  RVNSALHFESGVLFARMRFIFERILFFGKSD-IPEDRVEYVQKSYELLED  143
```

Secondary structure labels (bottom): H4 H5

Secondary structure labels (top): H6 H7

```
AaGSTd3    138  FLTERSYAAA-DHLTVADICLLGSVTALN-WLKYDLEPFPHIKGWVARVT  185
AdGSTd4-4  148  FLEGEQYVAGGDDPTIADLSILATIATYE-VAGYDLRRYENVQRWYERTS  196
AgGSTd1-6  140  FLEGQEYAAG-NDLTIADLSLAATIATYE-VAGFDFAPYPNVAAWFARCK  187
DmGSTd1    141  FLEGQDYAAG-DSLTVADIALVATVSTFE-VAKFEISKYANVNRWYENAK  188
BmGSTd     142  FLEGQKYVAG-PNLTVADLSLIASVSSLE-ASDIDFKKYANVKRWYETVK  189
LmGSTd1    143  FLEGSDWVAG-NSITIADYTIMASVSTAE-IIGFDIKFPKVAAWFEKAK  190
NlGSTd     142  FLEKSAFVAG-EDLTLADLAIVASISTIE-AVEYDLSPYKNINSWYSKVK  189
AfGSTe2    144  TLKD-DFVAG-SKMTIADFSCISTISSIMGVVPLEQSEHPRIYEWIDRLK  191
AaGSTe2    144  TLVD-DFVAG-PTMTIADFSCISTISSIMGVVPLEQSKHPRIYAWIDRLK  191
```

Secondary structure labels (bottom): H6 H7

Secondary structure labels (top): H8

```
AaGSTd3    186  GEIPDYAEFRKDVEEATKAYVVSKK------  210
AdGSTd4-4  197  AIVPGADKN-VEGAKVFGRYFTQK----    219
AgGSTd1-6  188  ANAPGYALN-QAGADEFKAKFLS--------  209
DmGSTd1    189  KVTPGWEEN-WAGCLEFKKYFE---------  209
BmGSTd     190  STAPGYQEANEKGLEAFKGLVNSMLKK----  216
LmGSTd1    191  KEIPSYEETNHAGALEFKKLFDSMTAKK----  218
NlGSTd     190  AAAPGYKEANEEGAKGFGQMFKAMTGK----  216
AfGSTe2    191  -QLPYYEEANGGGGTDLGKFVLAKKEENAKA  221
AaGSTe2    191  -QLPYYEEANGGGGTDLGKFVLAKKEENAKA  221
```

Secondary structure labels (bottom): H8

982

983